International Journal of Biochemistry and Cell Biology 154 (2023) 106332

Contents lists available at ScienceDirect

International Journal of Biochemistry and Cell Biology

journal homepage: www.elsevier.com/locate/biocel

Regulation of human *ZNF687*, a gene associated with Paget's disease of bone

Débora Varela [a,b], Tatiana Varela [a,b], Natércia Conceição [a,c,*], M. Leonor Cancela [a,c,*]

[a] Centre of Marine Sciences, University of Algarve, Faro, Portugal
[b] Faculty of Medicine and Biomedical Sciences, University of Algarve, Faro, Portugal
[c] Algarve Biomedical Center, University of Algarve, Faro, Portugal

ARTICLE INFO

Keywords:
ZNF687
Promoters
Regulation
Transcription factors
Methylation
Paget's disease of bone

ABSTRACT

Mutations in Zinc finger 687 (*ZNF687*) were associated with Paget's disease of bone (PDB), a disease characterized by increased bone resorption and excessive bone formation. It was suggested that *ZNF687* plays a role in bone differentiation and development. However, the mechanisms involved in *ZNF687* regulation remain unknown. This study aimed to obtain novel knowledge regarding *ZNF687* transcriptional and epigenetic regulation. Through *in silico* analysis, we hypothesized three *ZNF687* promoter regions located upstream exon 1 A, 1B, and 1 C and denominated promoter regions 1, 2, and 3, respectively. Their functionality was confirmed by luciferase activity assays and positive/negative regulatory regions were identified using promoter deletions constructs. *In silico* analysis revealed a high density of CpG islands in these promoter regions and *in vitro* methylation suppressed promoters' activity. Using bioinformatic approaches, bone-associated transcription factor binding sites containing CpG dinucleotides were identified, including those for NFκB, PU.1, DLX5, and SOX9. By co-transfection in HEK293 and hFOB cells, we found that DLX5 specifically activated *ZNF687* promoter region 1, and its methylation impaired DLX5-driven promoter stimulation. NFκB repressed and activated promoter regions 1 and 2, respectively, and these activities were affected by methylation. PU.1 induced *ZNF687* promoter region 1 which was affected by methylation. SOX9 differentially regulated *ZNF687* promoters in HEK293 and hFOB cells that were impaired after methylation. In conclusion, this study provides novel insights into *ZNF687* regulation by demonstrating that NFκB, PU.1, DLX5, and SOX9 are regulators of *ZNF687* promoters, and DNA methylation influences their activity. The contribution of the dysregulation of these mechanisms in PDB should be further elucidated.

1. Introduction

The C2H2-type zinc finger proteins (ZNFs) are the largest and best-characterized class of zinc finger family of transcription factors (TFs) in humans (Mackeh et al., 2018; Razin et al., 2012). They contain multiple Cys2-His2 (C2H2) motifs, the most common DNA-binding regions found in eukaryotic TFs and many of them highly conserved throughout evolution, indicating an essential role in important biological mechanisms such as gene transcriptional regulation (Fedotova et al., 2017). The zinc finger 687 (*ZNF687*) gene encodes a protein belonging to that family that is expressed in several tissues, such as bone (Divisato et al., 2016). Although not much is known concerning its function, mutations in *ZNF687* have been associated with a severe form of Paget's Disease of Bone (PDB) (Divisato et al., 2016). This disease is the second most common metabolic bone condition and is characterized by increased bone reabsorption by numerous, giant, and hyperactive osteoclasts followed by abnormal and excessive bone formation by the osteoblasts (Kaplan and Singer, 1995; Theodorou et al., 2011). As a result, affected bones of PDB patients are disorganized, enlarged, and deformed, therefore prone to fracture (Kaplan and Singer, 1995).

Diverse ZNF proteins are known to be important regulators of skeletal development/maintenance (Ganss and Jheon, 2004), yet the exact function of ZNF687 in bone metabolism is poorly understood. *In vitro* and *in vivo* studies indicate that ZNF687 has bone regulatory properties, being upregulated during osteoblast and osteoclast differentiation, and highly expressed during the regeneration of caudal fins in zebrafish, suggesting a role in bone cell proliferation and differentiation (Divisato et al., 2016). Furthermore, *ZNF687* was overexpressed in peripheral

* Corresponding authors at: Centre of Marine Sciences, University of Algarve, Faro, Portugal.
E-mail addresses: nconcei@ualg.pt (N. Conceição), lcancela@ualg.pt (M.L. Cancela).

https://doi.org/10.1016/j.biocel.2022.106332
Received 1 June 2022; Received in revised form 31 October 2022; Accepted 8 November 2022
Available online 11 November 2022

blood mononuclear cells (PBMC) samples derived from PDB-affected individuals (Divisato et al., 2016). Thus, it is crucial to gain further insights into the mechanisms involved in *ZNF687* regulation to better understand the pathogenesis of PDB.

Transcription factors and epigenetic modifications play crucial roles in the regulation of gene expression, therefore playing important regulatory roles in several biological processes (Liu et al., 2015). Epigenetics is defined as heritable changes in gene expression that occur without alterations in DNA sequence, including DNA methylation, histone modification, and non-coding RNAs (Probst et al., 2009). Emerging evidence suggests that perturbations in transcriptional regulation and epigenetic mechanisms affect the function/activity of bone cells and consequently, contribute to the pathogenesis of bone diseases (Xu et al., 2021; Vrtačnik et al., 2014; Park-Min, 2017; Sharma et al., 2020).

Since the mechanisms involved in *ZNF687* regulation remain unknown, the main objective of this work was to obtain novel knowledge regarding *ZNF687* transcriptional and epigenetic regulation, to understand the molecular mechanisms regulating its expression. For that, we characterized the putative *ZNF687* promoters and analyzed the functionality of binding sites for bone-related transcription factors overlapping CpG sites located on the *ZNF687* promoters and the effect of CpG methylation on its transcription.

2. Materials and methods

2.1. Collection of ZNF687 gene and transcripts sequences

Nucleotide sequences of the human *ZNF687* gene and its annotated and predicted transcript variants were retrieved from National Center for Biotechnology Information (NCBI) nucleotide database (www.ncbi.nlm.nih.gov). The structure of the transcripts was determined through the alignment of each transcript against the *ZNF687* genomic sequence using the Splign tool available at NCBI.

2.2. In silico analysis of ZNF687 promoters

The human *ZNF687* sequences upstream exon 1A, exon 1B and exon 1C (hence referred to as promoter regions 1, 2, and 3, respectively) were obtained from NCBI (accession number: NG_051575.1). The CpG islands present in the *ZNF687* gene were identified using the MethPrimer software (http://www.urogene.org/methprimer2/) with the default parameter values (CpG island length >100 bp, CG% > 50 %, and Obs/Exp > 0.6). The existence of regulatory motifs in the promoter regions was investigated through the Eukaryotic Promoter Database (https://epd.epfl.ch) and the Softberry program (www.softberry.com). The putative transcription factor binding sites (TFBSs) in *ZNF687* promoter regions were predicted using different web tools: Jaspar (www.jaspar.binf.ku.dk) with a relative profile score threshold of 80 %; lasagna (https://biogrid-lasagna.engr.uconn.edu/) with a cutoff p-value of 0.01 %; and Contra V3 (www.bioit.dmbr.ugent.be) with the core stringency of 0.95 and similarity matrix of 0.85.

2.3. Amplification of human ZNF687 promoter fragments

Three fragments of promoter region 1 (F5, F1, F6) and promoter region 2 (F2, F7, F8), and two fragments of promoter region 3 (F9, F10, F11) were amplified by polymerase chain reaction (PCR).

All fragments were amplified from HEK293 genomic DNA using specific primers and KAPA High Fidelity DNA polymerase enzyme (1 U/μl; Kapa Biosystems) according to the manufacturer's recommendations. Primer sequences are listed in Table 1. The PCR reactions were performed on a 2720 Thermal Cycler (Applied Biosystems) and the conditions applied were 95ºC for 3 min for initial denaturation, followed by 35 cycles under the following conditions: denaturation at 98ºC for 20 s, annealing at 55ºC for 15 s and extension at 72ºC for 1 min; and a final step of extension at 72ºC for 3 min. The PCR products were inserted into a pCRII-TOPO plasmid (Invitrogen) and constructs were confirmed by sequencing (CCMAR facility).

Table 1
List of primers used to amplify and clone human *ZNF687* promoter regions. Underlined sequences indicate the endonucleases restriction site. Fw: forward; Rev: reverse.

Name	Sequence (5′−3′)
Promoter amplification primers	
HsZNF687_F5_Fw	GGTTGGTTACATCGGGTTAGGG
HsZNF687_F1_Fw	AGGCAGGAGAATGGCGTGAA
HsZNF687_F6_Fw	TTCTGCCAGTGAGTGCTATTAGAG
HsZNF687_Rev1	GGAGCATGGAAGGAATCGGG
HsZNF687_F8_Fw	CTTGCCCAATGAGCATAAGAGGAC
HsZNF687_F7_Fw	GACCTACACTTCTGTGCTCCAC
HsZNF687_F2_Fw	ATTCCTTCCATGCTCCAAATCC
HsZNF687_Rev2	CACGCTTACTTGTTCCGCTC
HsZNF687_F9_Fw	GGTAAATACCCGCCCTTGGCT
HsZNF687_F10_Fw	GGAGATTGAAGGCTGCGGGA
HsZNF687_F11_Fw	ATCAGTCTCCAGTCTCTAGCGA
HsZNF687_Rev5	ACGGAATTAAGTCCCTGCCATCTG
pGL3-basic cloning primers	
HsZNF687_F7_Fw_*Kpn*I	AC**GGTACC**GACCTACACTTCTGTGCTCCAC
HsZNF687_Rev2_*Bgl*II	CG**AGATCT**CACGCTTACTTGTTCCGCTC
HsZNF687_F9_Fw_*Kpn*I	AC**GGTACC**GGTAAATACCCGCCCTTGGCT
HsZNF687_F10_Fw_ *Kpn*I	AC**GGTACC**GGAGATTGAAGGCTGCGGGA
HsZNF687_F11_Fw_ *Kpn*I	AC**GGTACC**ATCAGTCTCCAGTCTCTAGCGA
HsZNF687_Rev5_*Bgl*II	GG**AGATCT**ACGGAATTAAGTCCCTGCCATCTG
pCpGL-basic cloning primers	
HsZNF687_F5_Fw_*Bam*HI	CG**GGATCC**GGTTGGTTACATCGGGTTAGGG
HsZNF687_F1_Fw_*Bam*HI	CG**GGATCC**AGGCAGGAGAATGGCGTGAA
HsZNF687_F6_Fw_*Bam*HI	CG**GGATCC**TTCTGCCAGTGAGTGCTATTAGAG
HsZNF687_Rev1_*Nco*I	GACT**CCATGG**GGAGCATGGAAGGAATCGGG
HsZNF687_F8_Fw_*Bam*HI	CG**GGATCC**CTTGCCCAATGAGCATAAGAGGAC
HsZNF687_F7_Fw_*Bam*HI	CG**GGATCC**GACCTACACTTCTGTGCTCCAC
HsZNF687_F2_Fw_*Bam*HI	CG**GGATCC**ATTCCTTCCATGCTCCAAATCC
HsZNF687_Rev2_*Nco*I	GACT**CCATGG**CACGCTTACTTGTTCCGCTC
HsZNF687_F9_Fw_*Bam*HI	CG**GGATCC**GGTAAATACCCGCCCTTGGCT
HsZNF687_F10_Fw_*Bam*HI	CG**GGATCC**GGAGATTGAAGGCTGCGGGA
HsZNF687_F11_Fw_*Bam*HI	CG**GGATCC**ATCAGTCTCCAGTCTCTAGCGA
HsZNF687_Rev5_*Nco*I	GACT**CCATGG**ACGGAATTAAGTCCCTGCCATCTG

2.4. Cloning of human ZNF687 promoter fragments into pGL3-basic plasmid

ZNF687 promoter fragments were subcloned into the pGL3-basic luciferase reporter plasmid (Promega). For that, the pCRII-TOPO vector containing: i) the fragment F5 was double digested with *Kpn*I and *Xho*I, ii) the fragments F1 and F6 were digested with *Kpn*I and *Bgl*II, and iii) the fragments F2 and F8 were digested with *Hind*III and *Xho*I. Fragments F7, F9, F10, and F11 were reamplified from pCRII-TOPO using primers designed with *Kpn*I and *Bgl*II restriction sites (Table 1) and then digested with both endonucleases. Digested fragments were ligated into the pGL3-basic vector, previously digested with the same enzymes upstream of the firefly luciferase gene. All constructs were sequenced to confirm the fragments' proper insertion.

2.5. Preparation of methylated promoter-luciferase reporter constructs

To analyze the methylation effect in *ZNF687* transcriptional regulation, promoter fragments were also subcloned into the pCpGl-basic, a vector without CpGs on its backbone, which was kindly provided by Dr. Michael Rehli (University Hospital Regensburg, Germany). All fragments of promoter regions 1 and 2 were reamplified by PCR with primers containing *BamH*I and *Nco*I restriction sites (Table 1) and then double-digested with these endonucleases. Digested fragments were inserted into the pCpGL-basic upstream firefly luciferase gene. Constructs were methylated (Met) *in vitro* using the M.SssI methyltransferase

enzyme (NewEngland BioLabs), following the manufacturer's recommendations. Briefly, 7.5 μg of DNA plasmid was incubated with M.SssI enzyme (25 Units) in the presence of 1x NEB2 buffer and 640 μM S-Adenosylmethionine (SAM) at 37ºC for 2 h. The unmethylated DNA plasmid (Mock) was used as a control and treated as described above but without the M.SssI enzyme addition.

2.6. Transcription factor expression vectors

Expression vectors containing the cDNA of human *SOX9* (pcDNA3-SOX9), mouse *Dlx5* (pcDNA3.1-DLX5), and mouse *Pu.1* (pcDNA3-PU.1) were kindly provided by Dr. Dibyendu Kumar Panda (McGill University, Canada), Dr. Joseph Testa (Philadelphia, United States of America) and Dr. Rodney DeKoter (Western University, Canada), respectively. Since NFκB is present as a dimer of p65 and p50 in most cells, pCMV4-p65 and pCMV4-p50 vectors were purchased from Addgene (Cambridge, MA, USA) to mimic NFκB activity.

2.7. Cell culture maintenance

The Human Embryonic Kidney 293 cell line (HEK293; ATCC reference CRL-1573) was cultured in Dulbecco's Modified Eagle Medium (DMEM; Gibco) supplemented with 10 % fetal bovine serum (FBS; Invitrogen), 1 % penicillin (10,000 U/ml) and streptomycin (10,000 μg/ml) and 1 % L-Glutamine (200 mM). Cell cultures were maintained at 37 °C in a 5 % of CO_2 humidified atmosphere and sub-cultured every three-four days.

The human fetal osteoblast cell line (hFOB 1.19; ATCC reference CRL-11372) was cultured in Dulbecco's Modified Eagle Medium/Nutrient Mixture F-12 (DMEM/F-12; Gibco) containing 2.5 mM L-glutamine (without phenol red) and supplemented with 10 % FBS and 1 % penicillin/streptomycin. Cell cultures were maintained at 34ºC in a 5% CO_2 humidified atmosphere, and sub-cultured every three-four days.

2.8. Transient transfections

A day before transfections, 5×10^4 HEK293 cells or 3×10^4 hFOB cells per well were seeded in 24-well plates. At 50–60% of confluency, cells were transfected using a mixture containing 1 μl of X-treme GENE HP DNA Transfection reagent (Roche), 250 ng of promoter-luciferase constructs, 5 ng of pRL-null (*Renilla* luciferase vector; Promega) for HEK293 or 50 ng for hFOB, and medium without supplements to a final volume of 100 μl. For the co-transfections, 25 ng of either the TF-expressing vector or the empty vector was added. The final mixture was incubated for 15 min at room temperature and then divided into two wells, drop by drop. The plates were incubated at 37ºC for 48 h. The plasmids pGL3-Control or pCpGL-CMV and pGL3-basic or pCpGL-basic were also transfected and used as the positive and negative controls, respectively.

2.9. Luciferase reporter assays

After 48 h, cells were washed with cold phosphate-buffered saline and 100 μl of 1x passive lysis buffer (Biotium) was added. The Dual-Luciferase Reporter Assay kit (Promega) was used to determine Firefly and Renilla luciferase activities, according to the manufacturer's instructions. Bioluminescence was measured in a Synergy 4-Biotek microplate reader (Biotek). For normalization of luciferase activity, the ratio between Firefly and Renilla luciferase was calculated. At least three individual experiments were performed using duplicates.

In the co-transfection experiments, data are shown as fold change i.e., the ratio between the luciferase activity obtained by co-transfection of promoter constructs with the TF expression vectors and the luciferase activity obtained by co-transfection of promoter constructs with the empty expression vector.

2.10. Statistical analysis

Results are presented as the mean of luciferase activity ± standard deviation (SD). Statistical analysis was performed using GraphPad Prism 8.1.2 software. Significant differences between two and three groups were determined using unpaired t-test and one-way analysis of variance (ANOVA) followed by Tukey's post-test, respectively. The differences were considered statistically significant when $p < 0.05$.

3. Results

3.1. Structure of the human ZNF687 gene and its transcripts

The structure of the human *ZNF687* gene and the diversity of its transcripts were thoroughly searched using the NCBI database. *ZNF687* gene has 12 exons and 11 introns. Seven transcript variants resulting from alternative splicing were identified, of which three are known annotated transcripts and the other four are predicted transcript variants (Fig. 1). Structurally, the main differences among them are related to the 5′ region, while the region after exon 2 is similar in all of them (except for the sequence in exon 4 which is missing in predicted transcript variant 4). All transcript variants have the same translation initiation and termination sites (exon 2 and 9, respectively), except for the predicted transcript variant 1 whose translation site is located in exon 1A.

Since we found *ZNF687* transcripts starting at exon 1 A (NM_001304764.2, XM_005245366.4), exon 1B (NM_001304763.2, NM_020832.3, XM_011509813.2, XM_011509812.2) and exon 1C (XM_011509811.2), we raised the hypothesis that the corresponding regions upstream of each exon could operate as regulatory regions of *ZNF687* transcription. Therefore, we aimed to study the *ZNF687* transcriptional regulation driven by the areas upstream of exons 1A, 1B, and 1C, respectively denominated as Promoter Region 1 (PR1), Promoter Region 2 (PR2), and Promoter Region 3 (PR3).

3.2. In silico characterization of the regulatory regions of the human ZNF87 promoters

To gain insights into the transcriptional regulation of *ZNF687*, the presence of putative regulatory elements within the three promoter regions were investigated using several bioinformatics tools.

The presence of TATA-box sequences in promoters plays an important role in regulating the transcription of most genes. Although its position can vary slightly, it is typically located 25–35 bp upstream of the transcription start site (TSS) (Shi and Zhou, 2006). Our *in silico* analysis predicted a TATA-box sequence in both promoter regions 1 and 2, located a little further away than expected at positions − 129 and − 146, respectively (Fig. 2). The presence of a TATA-box motif was not predicted in promoter region 3, indicating a possible lower transcriptional activity.

The presence of putative TFBSs in promoter regions 1, 2, and 3 was identified using several prediction databases. Since it has been suggested a role for ZNF687 in bone-related pathways and its expression is dysregulated in PDB, the search was limited to TFs previously described as being associated with mechanisms related to bone diseases as well as with osteoclastogenesis and osteoblastogenesis. Among them, putative binding sites for NFκB (Nuclear Factor Kappa-B), SOX9 (SRY-box 9), DLX5 (Distal-Less Homeobox 5), and PU.1 (Purine-rich box 1) were identified in the different *ZNF687* promoter regions (Fig. 2). Further information regarding DNA sequences of the TFBSs and their location in the promoter regions are provided in Supplementary Fig. S1.

3.3. Functional characterization of the human ZNF87 promoters

To assess the ability of the three promoter regions to induce *ZNF687* transcription and further identify the regulatory active regions, the promoter fragments cloned in the pGL3-basic vector upstream of the

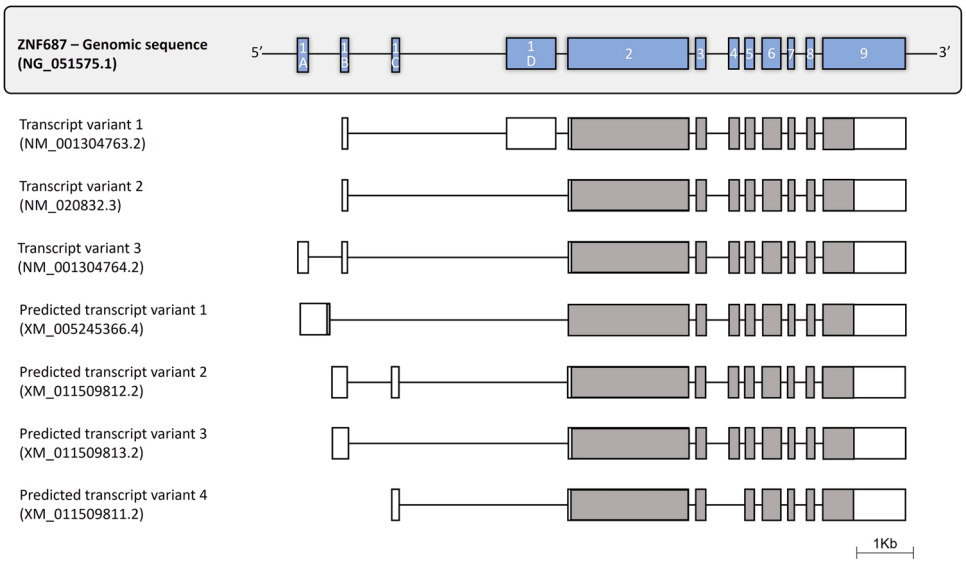

Fig. 1. Illustration of the structure of the *ZNF687* gene and its transcript variants. *ZNF6787* gene has twelve exons, and eight corresponding transcript variants were identified. In gene schematic representation, exons and introns are represented by boxes and lines, respectively. In transcripts schematic representation, the coding region is represented by gray boxes and the white boxes indicate the 5′ and 3′ untranslated regions. Both exons and introns are in scale.

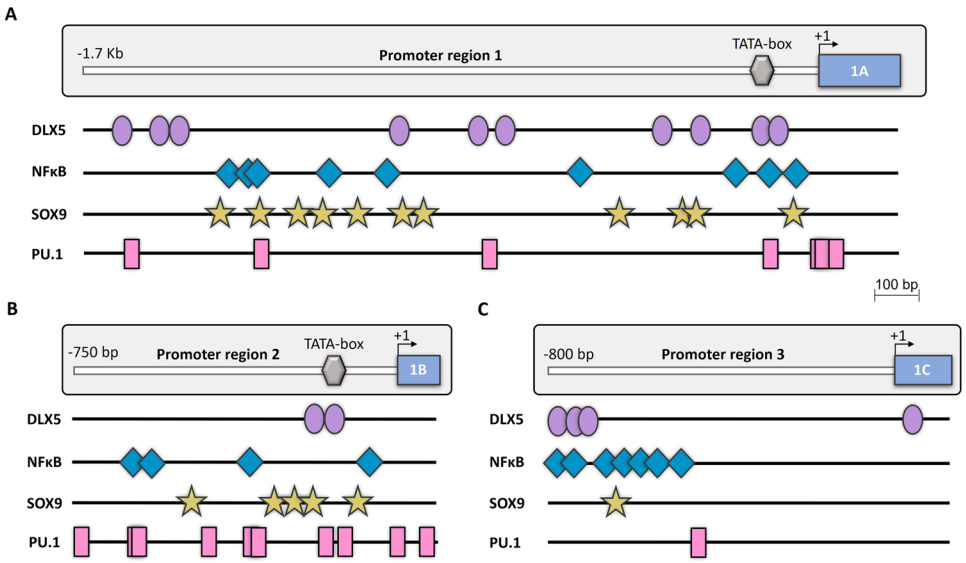

Fig. 2. Putative transcription factor binding sites in human *ZNF687* promoter regions. Regulatory elements in promoter region 1 (A), promoter region 2 (B), and promoter region 3 (C) were searched using several bioinformatics tools. Positions − 1.7 kb, − 750 bp, and − 800 bp are indicated according to the transcription start site (+1) in exon 1A, 1B, and 1C, respectively. TATA-box is represented by gray hexagons. Geometric shapes represent the transcription factor binding sites for DLX5 (oval), NFκB (diamonds), SOX9 (stars), and PU.1 (rectangles). Exons and promoter regions are in scale.

firefly luciferase cDNA were transfected into HEK293 cells, due to their high transfection efficiency. Concerning PR1, there was a 163-fold increase over pGL3-basic in the luciferase activity when the largest fragment (F5; −1632/+49) was transfected in HEK293 cells (Fig. 3A). When the region − 1632/− 913 was deleted, a significant decrease was observed in the promoter activity of F1 (−912/+49 fragment) compared to the activity of the F5 fragment, suggesting the presence of positive regulators in the region − 1632/− 913. Moreover, deletion of the region − 912/− 286 did not significantly affect the luciferase activity of F6 (fragment −285/+49) compared to the activity of F1. This could be the result of the binding of both activators and inhibitors within the deleted region or simply due to the lack of positive or negative regulatory elements in that region.

Relative luciferase activity of the largest fragment (F2; fragment −744/+106) of PR2 was approximately 82-fold higher than pGL3-basic activity and deletion of the region − 744/− 498 almost doubled this activity in F7 (fragment −497/+106), suggesting the presence of binding elements for negative regulators within the deleted region. In contrast, the deletion of the region − 497/− 197 resulted in a significant decrease in luciferase activity, indicating the existence of positive regulators in the eliminated sequence (Fig. 3B).

Regarding PR3, the relative luciferase activity of F9 (fragment −778/+50) was approximately 7-fold higher than that of pGL3-basic. Deletion of the region − 778/− 513 caused a significant decrease in the luciferase activity of F10 (fragment −512/+50), suggesting the presence of positive regulatory elements in the deleted region. Upon deletion of the region − 512/− 339 no significant alteration in the luciferase activity was observed (Fig. 3C).

Altogether, our results showed that all six fragments were able to induce luciferase transcription, although to different levels, being significantly higher when compared with the promoterless pGL3-basic vector, thus supporting our hypothesis that these promoter regions are functional and exhibit transcriptional activity. Interestingly, the basal activity of promoter region 3 was indeed noticeably lower when compared to promoter regions 1 and 2, possibly due to the lack of a TATA-box. This finding could indicate that the transcripts regulated by

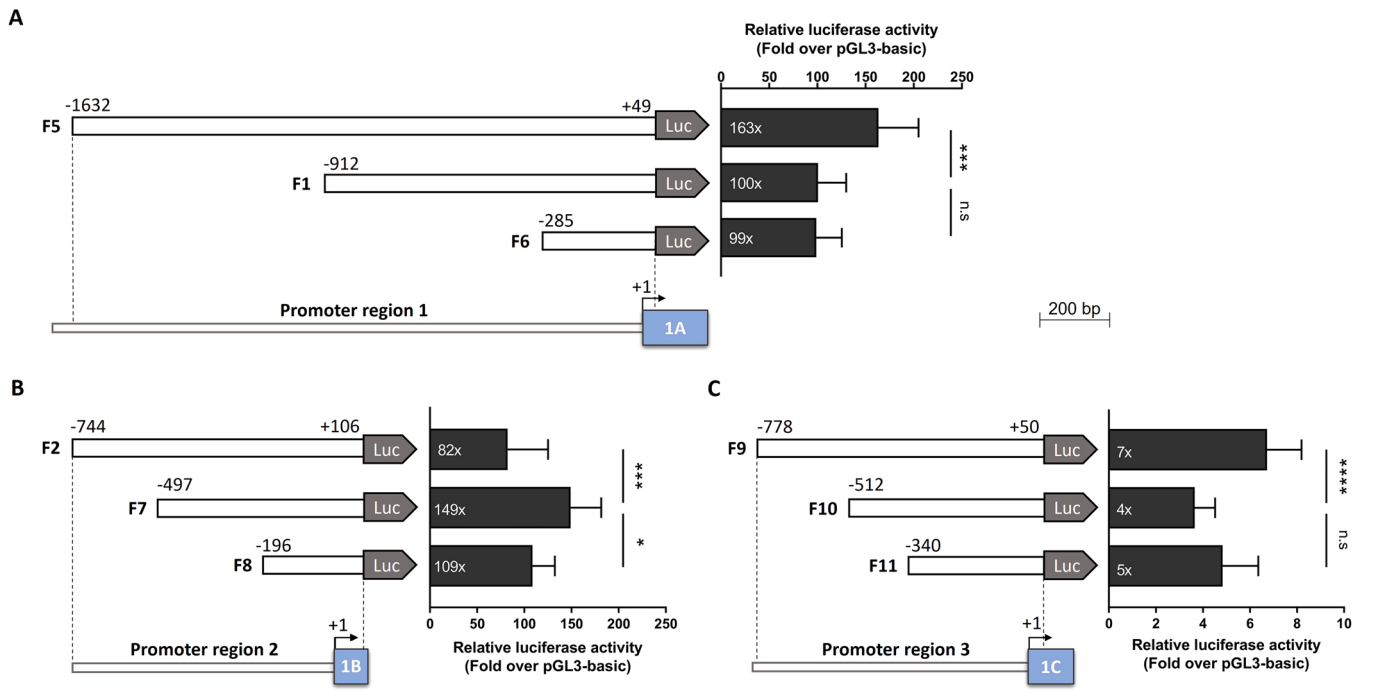

Fig. 3. Relative luciferase activity induced by *ZNF687* promoter regions in HEK293 cells. Fragments of promoter region 1 (A), promoter region 2 (B), and promoter region 3 (C) inserted in the pGL3-basic vector, upstream of the luciferase (Luc) gene, are represented by white boxes. Positions are indicated according to the respective transcription start site (+1). Luciferase activity is shown as fold change over pGL3-basic. Data are presented as the mean of luciferase activity ± SD. Statistical analysis was performed using a one-way analysis of variance followed by Tukey's post-test. * , * ** and * ** * indicate $p < 0.05$, $p < 0.001$ and $p < 0.0001$, respectively. n.s indicates no statistical difference. Exons and promoter regions are in scale.

promoter region 3 are less expressed.

3.4. Identification of CpG islands in the human ZNF687 gene

To investigate the role of the methylation in *ZNF687* transcription, the existence of CpG islands and CpG sites in the region from − 1632 upstream of the transcription start site in exon 1 A to the end of exon 1 C were analyzed through the MethPrimer software.

Bioinformatic analysis showed that the selected *ZNF687* genomic region has a high G-C content (>50 %) and it is rich in CpG islands, with a total of eleven predicted CpG islands (Fig. 4A). The CpG islands 1, 2, 3, 4, and 5 are located at positions − 1165/− 990, − 972/− 837, − 756/ − 653, − 305/− 187, and − 69/+ 182 relative to TSS of exon 1 A, respectively. CpG islands 6, 7, and 8 are located at positions − 466/ − 365, − 325/− 214, and − 149/+ 127 relative to TSS of exon 1B, respectively. Finally, CpG islands 9, 10, and 11 are located at positions − 597/− 404, − 401/− 216, and − 129/+ 28 relative to the TSS of exon 1 C, respectively. Additionally, *in silico* analysis showed that *ZF687* promoter regions are greatly enriched in CpG dinucleotides. A total of 320 CpG sites were identified and found to be evenly distributed in the analyzed *ZNF678* sequence. Moreover, several predicted binding sites for NFκB, PU.1, SOX9, and DLX5 comprise CpG dinucleotides.

All these findings suggest that DNA methylation may regulate the transcription of *ZNF687* by affecting the recruitment of the analyzed TFs to *ZNF87* promoter regions.

3.5. Effect of CpG methylation on ZNF687 promoter's activity

To assess the effect of CpG methylation on *ZNF687* transcription, methylated and non-methylated fragments of promoter regions 1 and 2 cloned into the pCpGL-basic vector were transfected into HEK293 cells and into an osteoblast cell line (hFOB). The pCpGL-Basic vector was chosen since its backbone lacks CpG dinucleotides, thus eliminating the artificial effects of reporter gene methylation. This analysis was not performed for promoter region 3 due to its lower activity compared to the other promoters.

Luciferase activities driven by *in vitro* methylated fragments of PR1 in HEK293 were approximately 95 % lower than the activities driven by the unmethylated fragments, and the same effect was observed for PR2 (Fig. 4B). Similar results were obtained when using hFOB cells, where a significant decrease in the luciferase activity was observed upon methylation of the fragments of both promoter regions (Fig. 4B). These results indicate that methylation of *ZNF687* promoter regions has a repressive effect on gene transcription probably by preventing the binding of several transcriptional activators.

3.6. Effect of transcription factors and methylation on ZNF687 transcriptional regulation

First, to investigate the capability of the selected bone-related transcription factors to stimulate and/or inhibit transcription of *ZNF687* and identify the potential binding sites responsible for this regulation, vectors expressing the TFs were co-transfected in HEK293 cells with the reporter constructs (cloned in the pGL3-basic) containing successive deletions of promoter regions 1 and 2.

Since methylation of CpG sites present in the *ZNF687* promoter could regulate its transcriptional activity by modulating the binding of the TFs, the vectors expressing the TFs were also co-transfected in HEK293 and hFOB cells with CpG-free reporter constructs (cloned in the pCpGL-basic) containing the largest fragment of PR1 and PR2, methylated (Met) or not (Mock).

3.6.1. NFκB regulates both ZNF687 promoters' activity and its function is impaired by methylation

Co-transfection of NFκB expressing vector with the largest fragment of *ZNF687* promoter region 1 (F5; −16332/+49) resulted in a significant 2-fold reduction of the luciferase activity (Fig. 5A), which was maintained upon deletion of − 1632/− 913 sequence, indicating that the

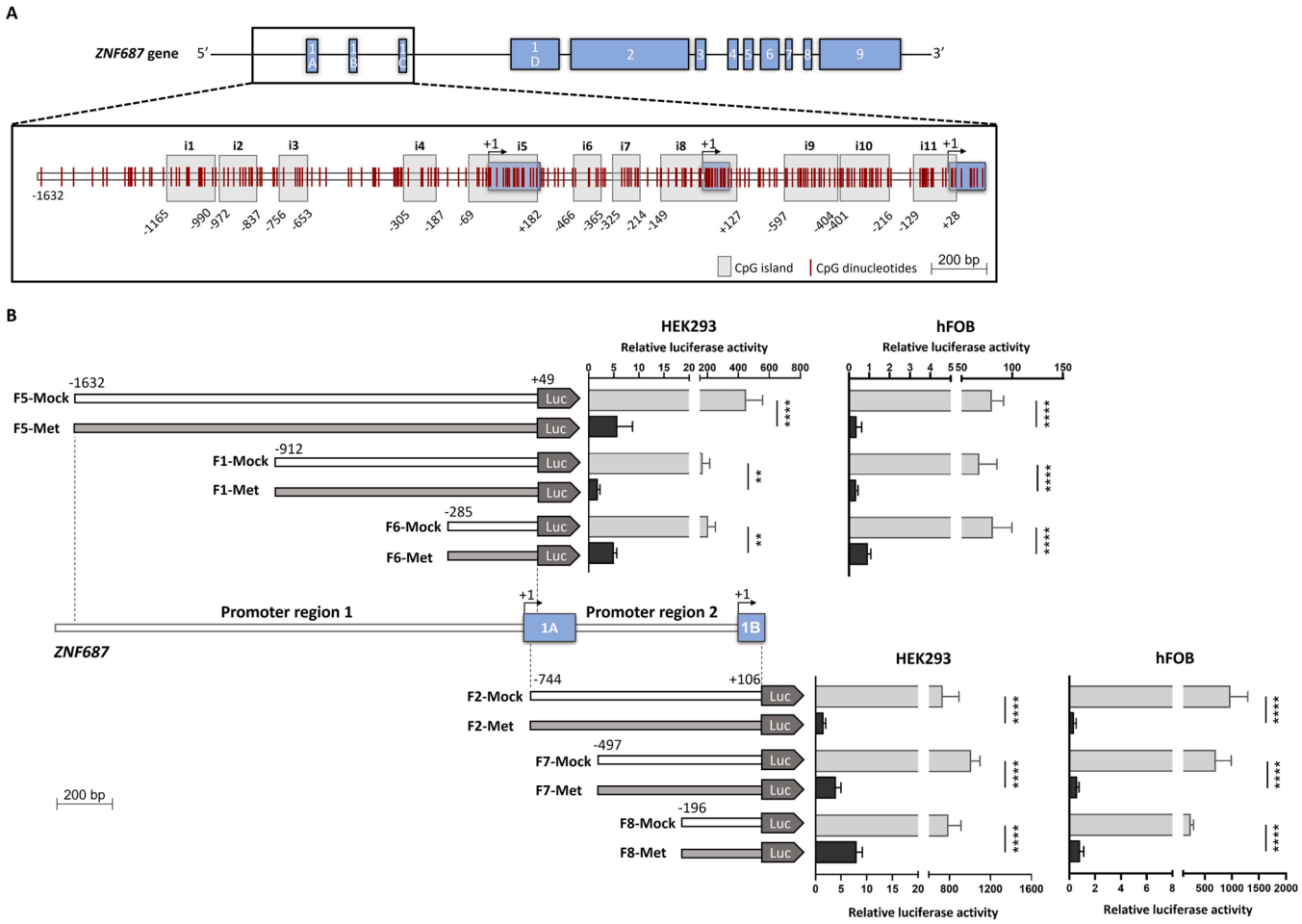

Fig. 4. Bioinformatics analysis of CpG in *ZNF687* and consequence of its methylation in promoter activity. (A) Schematic representation of CpG islands and CpG sites in *ZNF687* sequence from − 1632 relative to TSS in exon 1A to the end of exon 1C, determined using the MethPrimer program. The location of the CpG islands and CpG dinucleotides are identified by light gray boxes and vertical lines, respectively. (B) Effect of CpG methylation in the activity of *ZNF687* promoter regions 1 and 2 in HEK293 and hFOB cells. Non-methylated (Mock) and methylated (Met) promoter fragments inserted into the pCpGL-basic vector, upstream of the luciferase (Luc) gene, are represented by white and gray boxes, respectively. Start/end positions are indicated according to the respective transcription start site (+1). Data are presented as the mean of luciferase activity ± SD. * * and * ** * indicate $p < 0.01$ and $p < 0.0001$, respectively. Statistical analysis was performed using a one-way analysis of variance followed by Tukey's post-test.

four binding sites predicted within this region are probably not functional. Further elimination of the − 912/− 286 fragment significantly attenuated this reduction but not abolished it, suggesting that one or several putative TFBSs identified in the − 912/+ 49 region may be functional. In contrast, NFκB activated promoter region 2 by 1.6-fold upon co-transfection with the largest fragment (Fig. 5A). Deletion of the − 744/− 498 sequence did not impact promoter activity indicating that the two putative binding sites in this region are not functional. Successive elimination of the − 497/− 197 sequence caused a significant decrease in luciferase activity, suggesting that the predicted binding site at position − 349/− 337 could be functional. The fact that the stimulation of luciferase activity by NFκB was not abolished in the smallest fragment suggests that the binding site at position − 64/− 55 could also be functional.

NFκB co-transfections with the non-methylated CpG-free constructs containing the larger fragments of promoter regions 1 and 2 in HEK293 cells also inhibit and stimulated the luciferase activity, respectively, and the same trend was observed using hFOB cells thus confirming the previous results (Fig. 5B). Methylation of CpG sites in PR1 completely abolished the inhibition effect mediated by NFκB in both cell types, supporting our hypothesis that methylation affects the NFκB ability to bind *ZNF687* promoter region 1 and activate its transcription. CpG methylation of PR2 significantly attenuated the luciferase activity driven by NFκB in both cell types, indicating that methylation has also an impact on the activation of the *ZNF687* promoter region 2. The fact that the stimulation driven by NFκB was not abolished suggests that NFκB also binds to a sequence that does not overlap a CpG site, thus not affected by methylation. Interestingly, the putative binding site at position − 349/− 337 that we suggested to be functional does not comprise a CpG site.

Altogether, our results suggest that NFκB is a transcriptional regulator of *ZNF678* with a dual effect and CpG methylation impairs NFκB-driven *ZNF687* transcription.

3.6.2. PU.1 is a positive regulator of ZNF687 PR1 and its activity is impaired by methylation

Luciferase activity was significantly increased when PU.1 expression vector was co-transfected with constructs of promoter region 1 or promoter region 2 (Fig. 6A). In PR1, PU.1 enhanced the luciferase activity of the F5 fragment (−1632/+49) by 1.5-fold and this activity remained unchanged when further deletions were performed, suggesting that one or more of the four predicted binding sites located in the − 285/+ 49 sequence may be functional. Similarly, an increase in the luciferase activity of the largest fragment of PR2 (−744/+106) was observed upon co-transfection with the expression vector carrying PU.1. Subsequent deletion of the − 744/− 498 sequence did not alter the luciferase

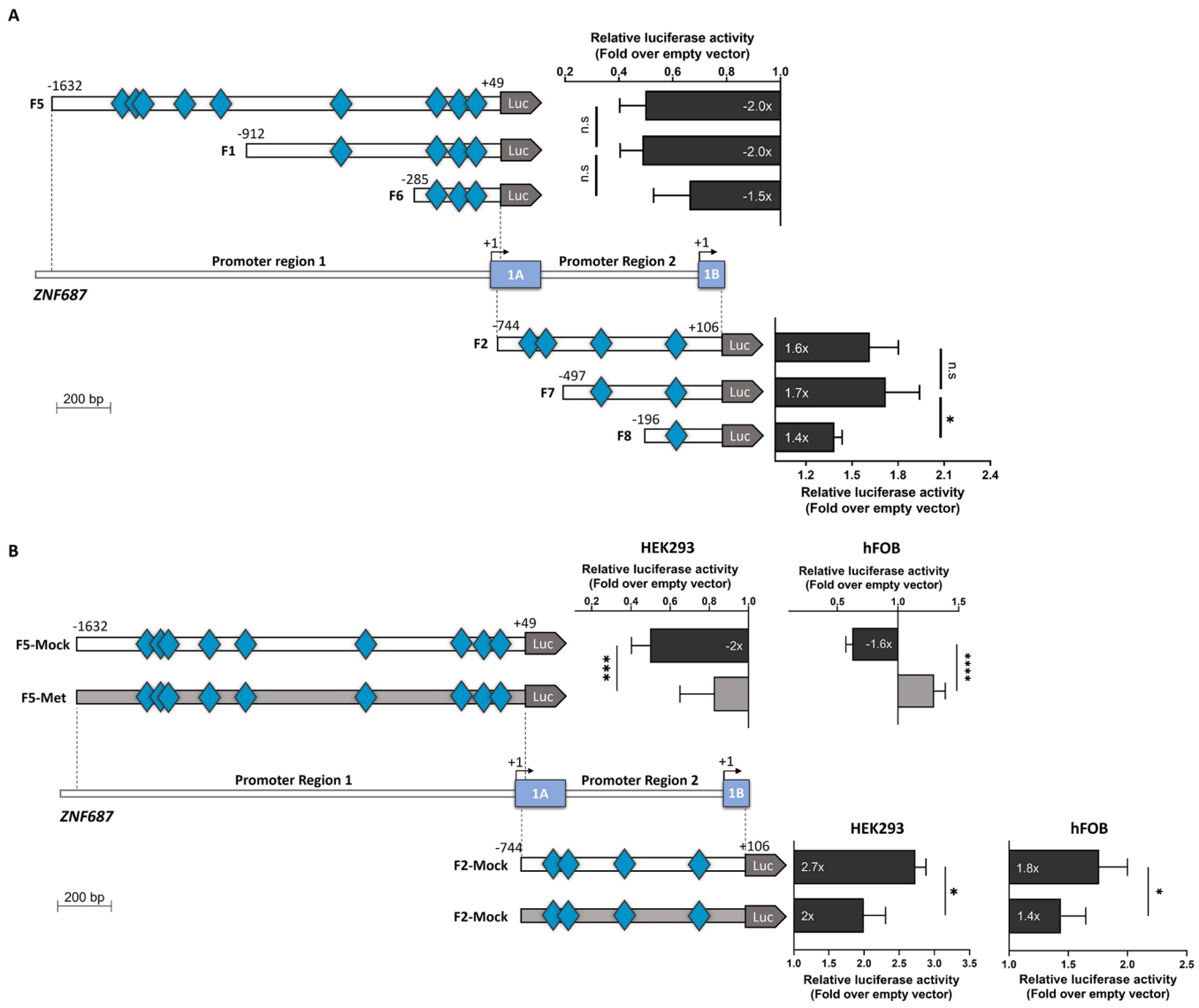

Fig. 5. Transcriptional regulation of *ZNF687* by NFκB and effect of the methylation. (A) Relative luciferase activity of *ZNF687* promoter regions 1 and 2 driven by NFκB in HEK293 cells. Fragments inserted into the pGL3-basic vector, upstream of the luciferase (Luc) gene, are represented by white boxes. Luciferase activity is shown as fold change over the pGL3-basic empty vector. (B) Effect of CpG methylation in the activity of *ZNF687* promoter regions 1 and 2 driven by NFκB in HEK293 and hFOB cells. Non-methylated (Mock) and methylated (Met) promoter fragments inserted into the pCpGL-basic vector, upstream of the luciferase (Luc) gene, are represented by white and gray boxes, respectively. Luciferase activity is shown as fold change over the pCpGL-basic empty vector. Fragments' start/end positions are indicated according to the respective transcription start site (+1). Diamonds indicate NFκB putative binding sites. Data are presented as the mean of luciferase activity ± SD. Black and gray bars represent values that are and are not significantly different, respectively, from the activity driven by the empty expression vector. Statistical analysis was performed using an unpaired t-test for two groups and a one-way analysis of variance followed by Tukey's post-test for three groups. * , * ** and * ** * indicate $p < 0.05$, $p < 0.001$ and $p < 0.0001$, respectively. N.s indicates no statistical difference. Exons and promoter regions are in scale.

activity indicating that the three predicted binding sites in this region are likely not functional. In contrast, the removal of the − 497/− 197 sequence led to a significant decrease in the luciferase activity to a basal level, suggesting that at least one of the three predicted binding sites within the deleted sequence could be functional.

Similarly, co-transfections of PU.1 and the non-methylated CpG-free construct harboring the largest fragment of PR1 (F5) in HEK293 and hFOB cells also significantly induced luciferase activity (Fig. 6B). In both cell types, CpG methylation significantly reduced the positive effect exerted by PU.1 in promoter region 1, indicating that PU.1 capability to bind *ZNF687* PR1 and activate its transcription is compromised by methylation. This stimulation was not abolished, suggesting that PU.1 also binds to a sequence that does not overlap a CpG site, therefore not affected by methylation.

Co-transfections of PU.1 and the non-methylated CpG-free construct harboring the largest fragment of PR2 (F2) in HEK293 resulted in a significant increase in the luciferase activity, which is in line with our previous results. This stimulation was not significantly affected by methylation. However, an opposite effect was observed in hFOB cells, where PU.1 significantly decreased the luciferase activity of F2-Mock and upon methylation this inhibition was abolished. Therefore, these results suggest that PU.1 regulates *ZNF687* promoter region 2 activity but depending on the cellular context it can act as an activator or repressor of transcription and be either affected or not by methylation.

3.6.3. DLX5 specifically enhances ZNF687 PR1 activity that is impaired by methylation

Co-transfection of the expressing vector carrying the DLX5 in HEK293 cells triggered a significant increase in the luciferase activity of PR1 (Fig. 7A). DLX5 enhanced the luciferase activity of F5 by 1.6-fold

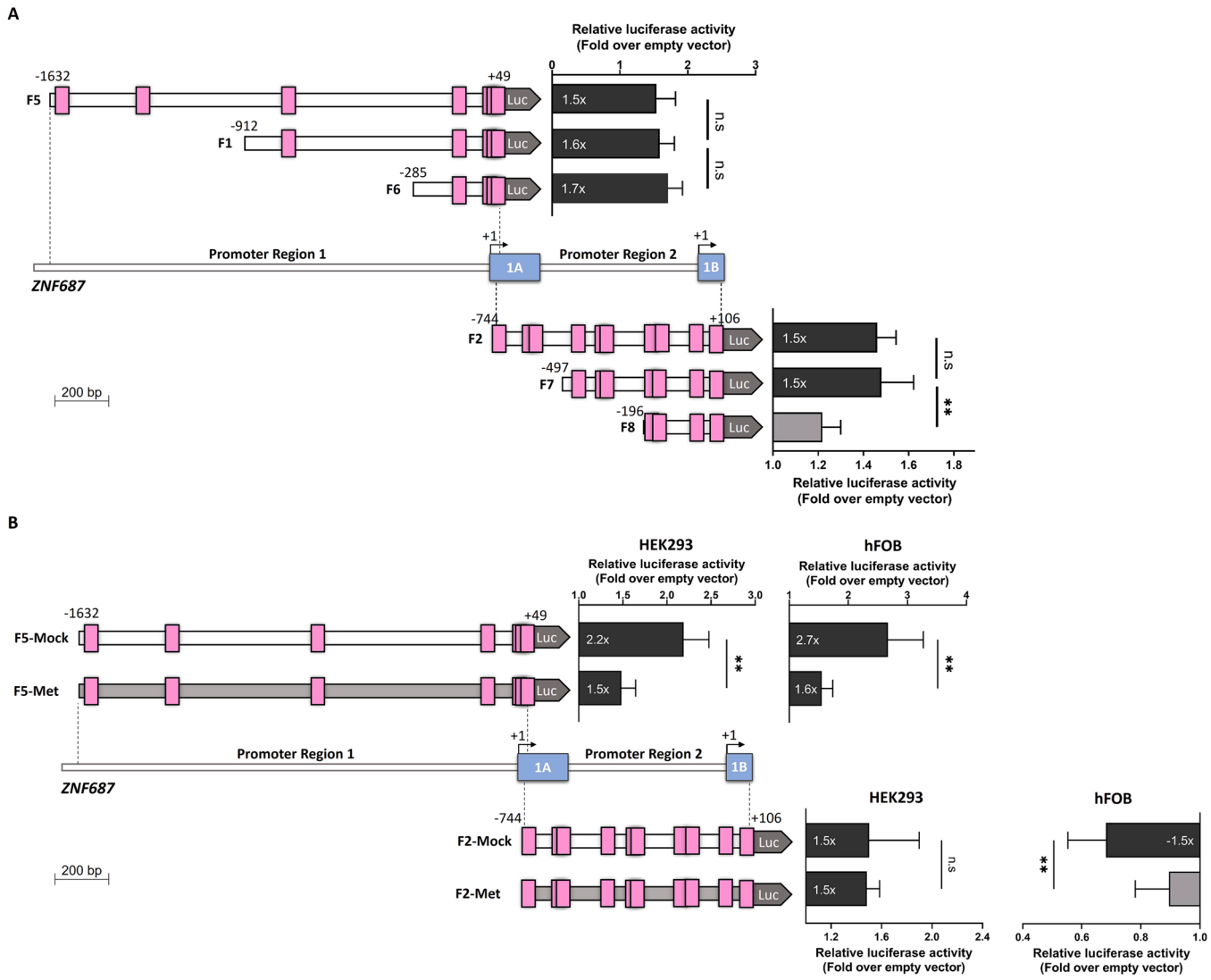

Fig. 6. Transcriptional regulation of *ZNF687* by PU.1 and effect of the methylation. (A) Relative luciferase activity of *ZNF687* promoter regions 1 and 2 driven by PU.1 in HEK293 cells. Fragments inserted into the pGL3-basic vector, upstream of the luciferase (Luc) gene, are represented by white boxes. Luciferase activity is shown as fold change over the pGL3-basic empty vector. (B) Effect of CpG methylation in the activity of the *ZNF687* promoter regions 1 and 2 driven by PU.1 in HEK293 and hFOB cells. Non-methylated (Mock) and methylated (Met) promoter fragments inserted into the pCpGL-basic vector, upstream of the luciferase (Luc) gene, are represented by white and gray boxes, respectively. Luciferase activity is shown as fold change over the pCpGL empty vector. Fragments' start/end positions are indicated according to the respective transcription start site (+1). Rectangles indicate PU.1 putative binding sites. Data are presented as the mean of luciferase activity ± SD. Black and gray bars represent values that are and are not significantly different, respectively, from the activity driven by the empty expression vector. Statistical analysis was performed using an unpaired t-test for two groups and a one-way analysis of variance followed by Tukey's post-test for three groups. * * indicates $p < 0.01$ and n.s indicates no statistical difference. Exons and promoter regions are in scale.

and the elimination of the − 1632/− 913 sequence completely abolished DLX5 induction, suggesting that one or several of the four binding sites predicted within this sequence may be functional. It also indicates that the six binding sites predicted in the region − 912/+ 49 are not functional. Co-transfection of the expressing vector carrying the DLX5 had no significant effect on the luciferase activity of any constructs of PR2, indicating that the two predicted binding sites are most likely not functional (Fig. 7A).

In accordance, the DLX5 expressing vector when co-transfected in HEK293 cells with the unmethylated CpG-free plasmid carrying the F5 fragment of PR1 also significantly induced the luciferase activity (Fig. 7B). After CpG methylation, this stimulation driven by DLX5 in PR1 was abolished, indicating that DLX5 may bind to a sequence overlapping a CpG site, that when methylated prevents the transcription factor from carrying out its function, probably by becoming inaccessible to its binding. The same experiments using hFOB cells resulted in the same observations thus validating our findings.

Taken together, our results suggest that DLX5 is a positive transcriptional regulator of *ZNF687* promoter region 1 and CpG methylation impairs its biological activity.

3.6.4. SOX9 regulates both ZNF687 promoters' activity and it is affected by methylation

Co-transfection of the expressing vector carrying the SOX9 and both promoters 1 and 2 constructs in HEK293 cells resulted in a significant increase in the luciferase activity (Fig. 8A). In PR1, SOX9 stimulated the luciferase activity of the largest fragment by 1.8-fold, and subsequent deletions had no significant effect on this activity,suggesting that, of the eleven predicted binding sites in PR1, only one or both located in the − 285/+ 49 sequence could be functional. The same trend was observed for PR2, in which co-transfection of SOX9 with the largest fragment enhanced the luciferase activity by 2.1-fold and successive deletions

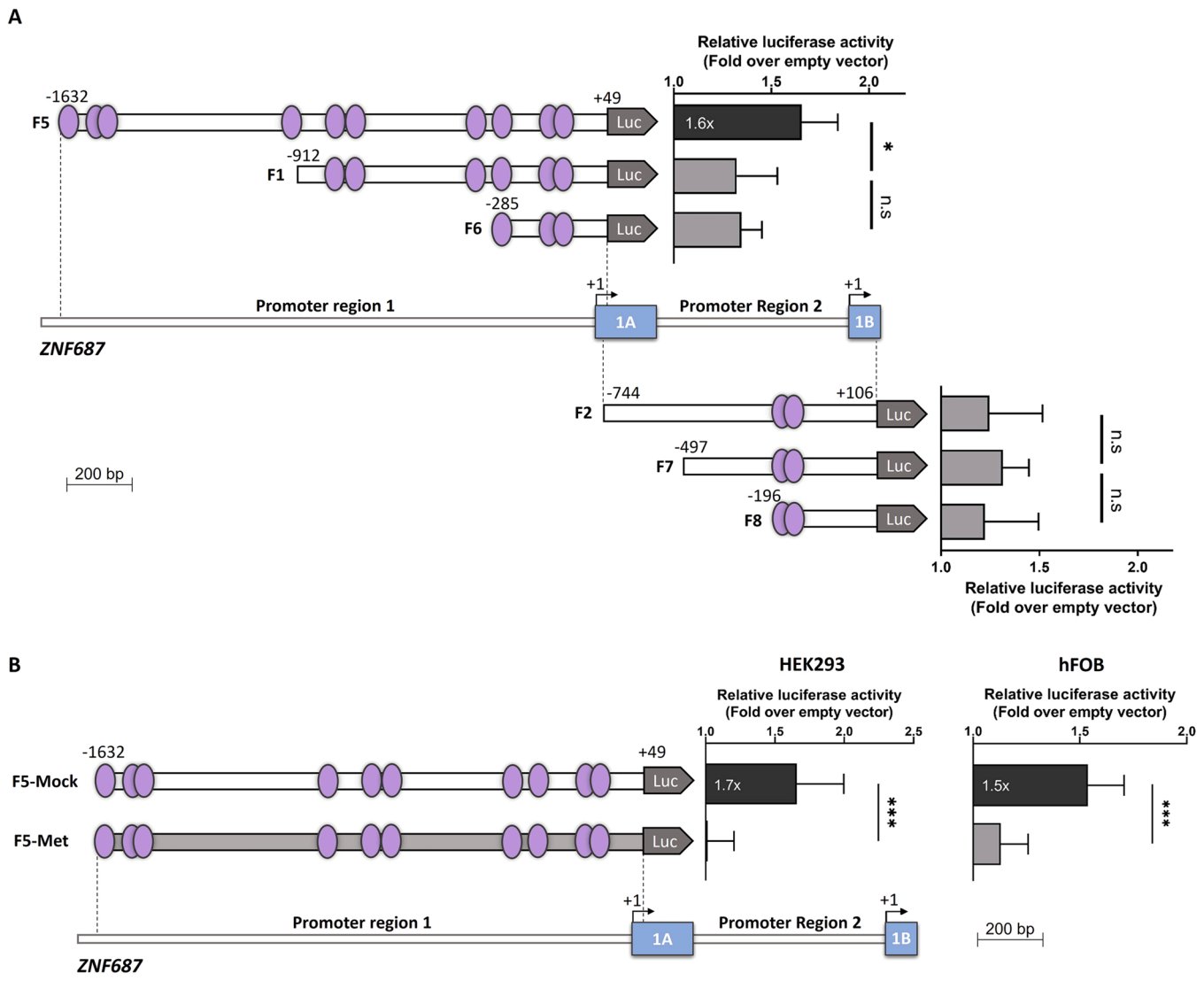

Fig. 7. Transcriptional regulation of *ZNF687* by DLX5 and effect of the methylation. (A) Relative luciferase activity of *ZNF687* promoter regions 1 and 2 driven by DLX5 in HEK293 cells. Fragments inserted into the pGL3-basic vector, upstream of the luciferase (Luc) gene, are represented by white boxes. Luciferase activity is shown as fold change over the pGL3-basic empty vector. (B) Effect of CpG methylation in the activity of *ZNF687* promoter region 1 driven by Dlx5 in HEK293 and hFOB cells. Non-methylated (Mock) and methylated (Met) promoter fragments inserted into the pCpGL-basic vector, upstream of the luciferase (Luc) gene, are represented by white and gray boxes, respectively. Luciferase activity is shown as fold change over the pCpGL-basic empty vector. Fragments' start/end positions are indicated according to the respective transcription start site (+1). Oval shapes indicate DLX5 putative binding sites. Data are presented as the mean of luciferase activity ± SD. Black and gray bars represent values that are and are not significantly different, respectively, from the activity driven by the empty expression vector. Statistical analysis was performed using an unpaired t-test for two groups and a one-way analysis of variance followed by Tukey's post-test for three groups. * and * ** indicate $p < 0.05$ and $p < 0.001$. n.s indicates no statistical difference. Exons and promoter regions are in scale.

caused no alteration in this activity. This indicates that of the five predicted binding sites in PR2 only one or both located in the − 196/+ 106 sequence may be functional.

The luciferase activity of the unmethylated CpG-free constructs containing the PR1 or PR2 largest fragments also significantly increased when co-transfected in HEK293 cells with the SOX9 expressing vector (Fig. 8B), thus confirming our previous results. Methylation of CpG sites of both promoters abolished the SOX9 stimulation, indicating that binding to the predicted sites in both PR1 and PR2 are compromised by changes in their accessibility caused by methylation. In contrast, PU.1 when co-transfected in hFOB cells exerted an opposite effect on both promoters, i.e., led to the inhibition of both PR1 and PR2 activity. Nevertheless, this regulation was also compromised by CpG methylation in both promoter regions.

Given our results, we propose that SOX9 acts as a transcriptional activator and repressor of both *ZNF687* promoter regions in HEK293 and hFOB cells, respectively, and this regulation is affected by CpG methylation.

4. Discussion

The zinc finger protein 687 is expressed in many tissues, including in bone where it was recently found to play a role in its metabolism (Divisato et al., 2016). Mutations in *ZNF687* were observed in individuals with Paget's disease of bone and its overexpression has been associated with PDB (Divisato et al., 2016). This disease has a significant genetic component associated. Mutations in the *SQSTM1* gene are the most frequent cause of PDB, occurring in up to 50 % of patients with PDB familial form (Gennari et al., 2019). In addition, several susceptibility genes with an important role in osteoclast differentiation have been discovered using genome-wide association studies, including *OPTN*, *CSF1*, *TNFRSF11 A*, and *DCSTAMP* (Gennari et al., 2019). Mutations in

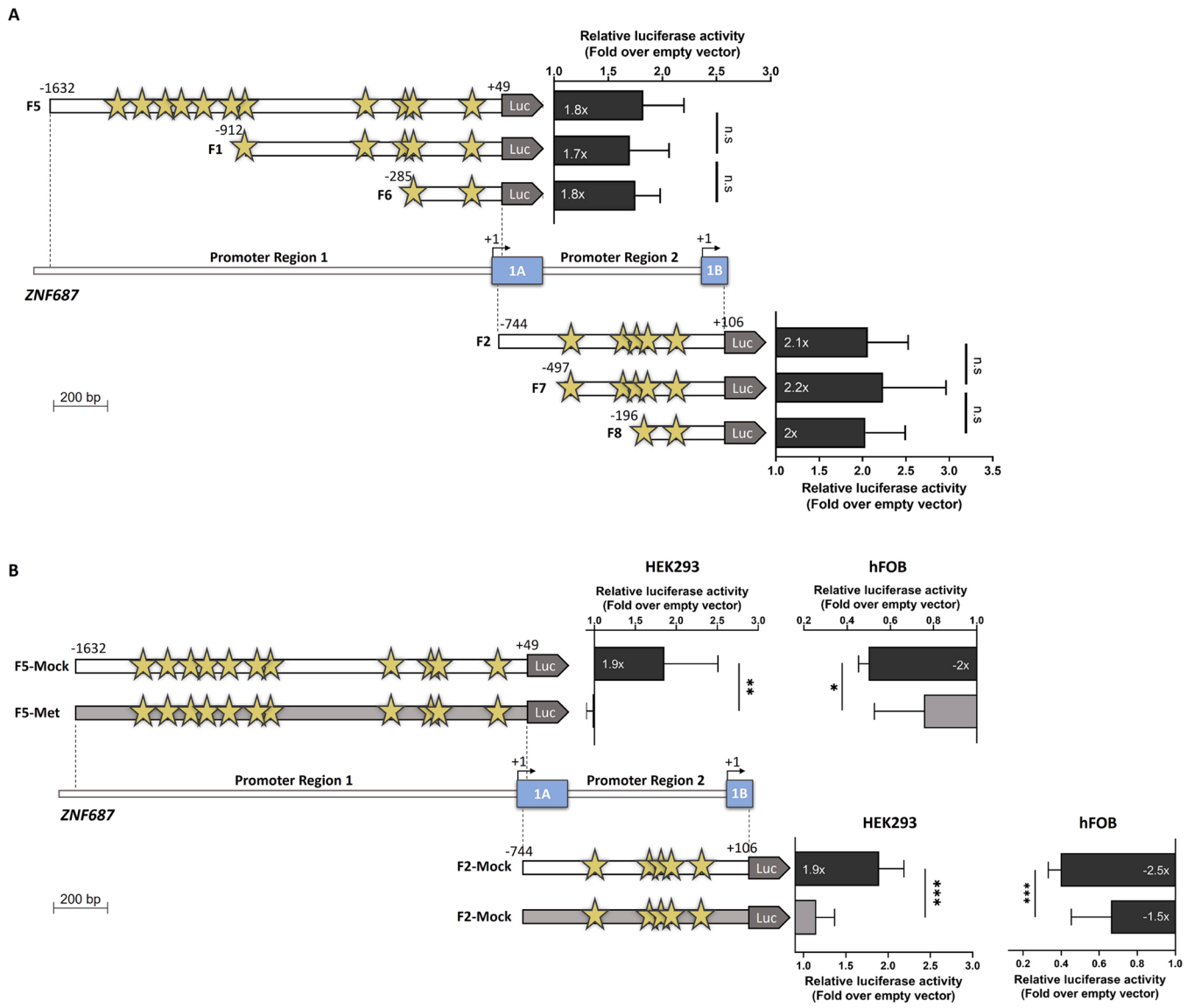

Fig. 8. Transcriptional regulation of *ZNF687* by SOX9 and effect of the methylation. (A) Relative luciferase activity of *ZNF687* promoter regions 1 and 2 driven by SOX9 in HEK293 cells. Fragments inserted into the pGL3-basic vector, upstream of the luciferase (Luc) gene, are represented by white boxes. Luciferase activity is shown as fold change over the pGL3-basic empty vector. (B) Effect of CpG methylation in the activity of the *ZNF687* promoter regions 1 and 2 driven by SOX9 in HEK293 and hFOB cells. Non-methylated (Mock) and methylated (Met) promoter fragments inserted into the pCpGL-basic vector, upstream of the luciferase (Luc) gene, are represented by white and gray boxes, respectively. Luciferase activity is shown as fold change over the pCpGL-basic empty vector. Fragments' start/end positions are indicated according to the respective transcription start site (+1). Stars indicate SOX9 putative binding sites. Data are presented as the mean of luciferase activity ± SD. Black and gray bars represent values that are and are not significantly different, respectively, from the activity driven by the empty expression vector. Statistical analysis was performed using an unpaired t-test and a one-way analysis of variance followed by Tukey's post-test for two and three groups, respectively. * , * * and * ** indicate $p < 0.05$, $p < 0.01$ and $p < 0.001$. n.s indicates no statistical difference. Exons and promoter regions are in scale.

ZNF687 have been associated with a severe form of PDB characterized by an early onset and multiple affected bones that are sometimes complicated by the development of giant cell tumor (GCT) (Gennari et al., 2022). More recently, the contribution of epigenetic determinants to PDB has been shown. Diboun et al. showed for the first time in 2021 that epigenetic factors are involved in the pathogenesis of PDB and may be used as diagnostic markers for disease prediction (Diboun et al., 2021). Many differentially methylated CpG sites were identified in PDB patients when compared to controls, of which several are located within or near genes implicated in bone remodeling (e.g *TAL1*, *MAF*, *ZIC1*) (Diboun et al., 2021). Emerging evidence indicates that epigenetic modification such as DNA methylation could be implicated in aging-bone diseases (Reppe et al., 2017; Visconti et al., 2021). However, no studies are available regarding the *ZNF687* transcriptional regulation and the impact of CpG methylation on the binding of transcription factors in its promoter regions. To the best of our knowledge, the present study provides the first data on *ZNF687* promoter regions functionality, *ZNF687* transcription activation or repression by bone-related transcription factors, and the effect of CpG methylation in the TFs-mediated *ZNF687* activity.

Functional analysis of the *ZNF687* promoter is required to understand the molecular mechanisms underlying *ZNF687* expression. We demonstrated that three putative promoter regions upstream of exon 1A, exon 1B, and exon 1C of the human *ZNF687* gene, which likely drives the transcription of the different transcripts, were found to be functional and several positive and negative regulatory regions were identified. These data indicate that the upregulation of *ZNF687* in PDB could be the result of the complex interactions among distinct regulatory elements acting

on different promoters. Nevertheless, promoter region 3 presented significantly less activity compared to the others, suggesting that the expression of the predicted transcript variant 4 regulated by this promoter may be lower or cell-type specific.

Regulation of gene expression by transcription factors, through the binding to the promoter of target genes, represents an essential mechanism in cell biology (Lee and Young, 2013). Several studies showed that DNA methylation of CpG dinucleotides has the potential to modulate the binding of transcription factors to gene promoters, thus playing a role in gene expression and regulation (Héberlé and Bardet, 2019). Based on the bioinformatics analysis, we showed that several putative binding sites for different transcription factors were predicted in human *ZNF687* promoter regions, including cis-regulatory elements associated with bone metabolism, such as NFκB, PU.1, DLX5, and SOX9. Additionally, a high abundance of CpG islands was also predicted in *ZNF687* promoter regions and several binding sites for these TFs were found to overlap or surround CpG dinucleotides, suggesting that they could be involved in the regulation of *ZNF687* expression and that CpG methylation could modulate *ZNF687* transcription. Therefore, we have investigated the effect of those TFs on promoter regions 1 and 2 and the impact of methylation in their activity, using two different cell types: the easily transfected HEK293 and the osteoblast hFOB cell lines. Similar data were obtained from the co-transfections of NFκB and Dlx5 with both promoter regions and PU.1 with PR1 using these two cell lines. In contrast, co-transfections of SOX9 with both PR1 and PR2 and PU.1 with PR2 resulted in opposite effects in HEK293 and hFOB cells. Studies have shown that TFs can act as transcriptional activator or repressor, depending on the cellular and promoter environment (Roberts and Green, 1995; Handy and Gavras, 1996). Since HEK293 and hFOB cells are originated from different tissues, the opposite effects may be related to the presence of distinct endogenously expressed TFs that can modulate the function of PU.1 and SOX9.

NFκB is a family of multifunctional transcriptional factors that regulate the expression of genes involved in many biological functions, including inflammation, differentiation, and cell growth (Oeckinghaus and Ghosh, 2009; Hayden and Ghosh, 2012). Additionally, NFκB also plays a role in skeletal development, endochondral ossification, osteoclast and osteoblast functions, and osteoclast differentiation (Yang and Karsenty, 2002; Datta et al., 2013; Novack, 2011). Although it is considered mostly as a transcriptional activator (Cun-Yu et al., 1979), NFκB also functions as a transcriptional repressor, depending on its dimerization partner (Datta et al., 2013; Zhang and Kone, 2002). Interestingly, we proposed that NFκB is a transcriptional regulator of *ZNF687* with a dual effect i.e., it negatively regulates *ZNF687* transcription by binding to the promoter region 1 while it positively regulates *ZNF687* transcription by binding to the promoter region 2. In this case, the NFκB dual function is probably related to the different promoter regions' context since the same results were obtained using both HEK293 and hFOB cells. Our data also suggest that CpG methylation affects the *ZNF687* transcription driven by NFκB. Accordingly, several studies reported that methylation of the NFκB binding site impacted gene expression (Rump et al., 2019; Wang et al., 2017).

PU.1 is a member of the ETS transcription factor family that has a key role in the development of hematopoietic cell lineages (Rothenberg et al., 2019). It plays a critical role in osteoclast differentiation by regulating *RANK* gene transcription (Kwon et al., 2005). Mouse models lacking PU.1 exhibit an osteopetrosis phenotype due to the developmental impairment of osteoclasts and macrophages (Tondravi et al., 1997). Our results suggest that in HEK293 cells, PU.1 is a positive regulator of *ZNF687* transcription by binding both promoter regions 1 and 2, while in hFOB cells it has a dual function, by positively and negatively regulating promoter regions 1 and 2, respectively. PU.1 is mainly recognized as a transcriptional activator of several genes such as *LIMD1*, *PF-2*, *RANK*, and *KLF4* (Kwon et al., 2005; Ramanathan et al., 2005; Foxler et al., 2011; Karpurapu et al., 2014) however it can also have a repressive role. It can interact with various regulatory factors that change PU.1 general transcriptional activity (Burda et al., 2010). Interestingly, it was shown that during osteoclastogenesis, PU.1 interacts with MITF to activate the transcription of *CTSK* and *ACP5*. However in myeloid precursors PU.1 can repress these same genes when EOS joins the complex (Rong et al., 2007). Furthermore, Karpurapu et al. showed that methylation of *KLF4* promoter attenuated the stimulation of its activity driven by PU.1, indicating a negative influence of methylation on PU.1 binding (Karpurapu et al., 2014). In our study, PU.1 ability to activate transcription was also impaired by CpG methylation.

Transcription factor DLX5, a member of the distal-less homeobox domain family, is expressed at the early stages of bone development and plays a crucial role in osteogenesis regulation (Samee et al., 2008; Tadic et al., 2002). Overexpression of *DLX5* is known to stimulate osteoblast differentiation (Tadic et al., 2002) and *Dlx5* homozygous mutant mice show a reduced bone volume as well as osteoblasts with lower proliferation and differentiation capacity (Samee et al., 2008). Dlx5 functions as a transcriptional activator of many genes, including *Runx2* and *c-MYC* (Lin et al., 2021; Lee et al., 2005). Here, we showed that Dlx5 is also a positive regulator of *ZNF687* transcription but specifically of promoter region 1, which may indicate distinctive spatial/temporal expression patterns of the different transcripts controlled by the two promoters during bone development. DNA methylation of promoter region 1 was shown to repress *ZNF687* transcription induced by Dlx5, possibly due to the blocking of its binding.

The transcription factor SOX9 plays a fundamental role in chondrogenesis during embryonic development (Lefebvre and Dvir-Ginzberg, 2017). The inactivation of this TF leads to abnormalities in cartilage and bone formation (Jiang et al., 2018) and its upregulation of SOX9 is also linked with the progression of osteosarcoma (Zhu et al., 2013). It has been reported that SOX9 has both activation and repression functions, depending on the promoter site where it binds and the factors with which interacts (Kamachi and Kondoh, 2013). SOX9 plays a crucial transcriptional role in chondrocytes as an activator of cartilage-specific genes, such as *Col2a1* (Lefebvre et al., 1997) and *COL9A1* (Imagawa et al., 2014). It also represses the transcription of the osteogenic glycoprotein *Spp1* (Peacock et al., 2011). Our results suggest that SOX9 is a transcriptional inducer and repressor of both *ZNF687* promoter regions 1 and 2 in HEK293 and hFOB, respectively. CpG methylation affects *ZNF687* transcription by blocking the binding sites of SOX9 within CpG dinucleotides in both cell lines. In agreement, it was reported that CpG methylation also impaired the SOX9-driven activation of the *COL9A1* promoter by altering the SOX9 binding to DNA (Imagawa et al., 2014).

Through sequential promoter deletions, we have identified several possible cis-regulatory elements for NFκB, PU.1, DLX5, and SOX9 transcription factors. Further experiments should be performed to confirm the functionality of these TFBSs, for instance by mutating the core sequence of each candidate binding site. Also, the physical interaction between the TFs and the putative sequences identified in *ZNF687* promoters should be proven by electrophoretic mobility shift assay and chromatin immunoprecipitation (CHIP). In the future, it would be important to validate our results using murine models since the use of a systems biology is crucial for a more comprehensive analysis of gene regulation.

There are no reports regarding *ZNF687* methylation status and bone diseases although other studies showed that *ZNF687* methylation is altered in other pathological conditions (e.g., multiple sclerosis and prostate cancer) (Celarain and Tomas-Roig, 2020; Berglund et al., 2022). Whether the alterations in the TFs expression and/or disturbance in *ZNF687* methylation/regulation are implicated in PDB pathophysiology should be further investigated. For that, and based on our work, future studies should be performed using samples from PDB individuals and healthy controls (e.g., PBMCs and osteoclast derived from PBMCs) to compare the expression of these TFs (by qPCR), the methylation status (by bisulfite direct sequencing) of *ZNF687* and the physical binding of TFs to *ZNF687* promoters (by CHIP).

Besides the epigenetics implications, the existence of variants in the gene promoter located on transcription factors binding sites and CpG sites can also alter gene regulation and expression. This effect was already shown for *OPTN*, with the functional analysis of the variant rs3829923 showing that the transcription factor E47 regulates *OPTN* gene expression only when the T allele is present (Silva et al., 2018). The genome resources databases shows that several SNPs are overlapping CpG sites located in *ZNF687* promoter regions 1 and 2. Therefore, in the future, these variants should be searched in PDB patients and compared to control individuals to identify if there is an association with the disease and, functional studies should be performed to further elucidate their potential role in disease development.

In conclusion, the present study identified three novel functional *ZNF687* promoters and provided new insights into the *ZNF687* transcriptional regulation by bone-associated TFs. We revealed that NFκB, PU.1, DLX5, and SOX9 play a regulatory role in the transcription of the human *ZNF687* gene. Furthermore, we found that *ZNF687* promoters are rich in CpG dinucleotides and CpG methylation regulates *ZNF687* transcription possibly by modulating the binding of the transcription factors to the promoters.

CRediT authorship contribution statement

Conceptualization, **Natércia Conceição** and **M. Leonor Cancela**; Formal analysis, **Débora Varela**; Funding acquisition, **M. Leonor Cancela**; Investigation, **Débora Varela**; Methodology, **Débora Varela, Tatiana Varela**; Project administration, **M. Leonor Cancela**; Resources, **Natércia Conceição** and **M. Leonor Cancela**; Supervision, **Natércia Conceição** and **M. Leonor Cancela**; Writing – original draft, **Débora Varela**; Writing – review & editing, **Natércia Conceição** and **M. Leonor Cancela**.

Conflict of interests

The authors declare no conflict of interest.

Data availability

Data will be made available on request.

Acknowledgements

This study received Portuguese national funds from FCT - Foundation for Science and Technology through projects UIDB/04326/2020, UIDP/04326/2020 and LA/P/0101/2020. Débora Varela and Tatiana Varela are recipients of a Ph.D. fellowship from FCT (SFRH/BD/141918/2018 and SFRH/BD/144230/2019, respectively).

Appendix A. Supporting information

Supplementary data associated with this article can be found in the online version at doi:10.1016/j.biocel.2022.106332.

References

Berglund, A., et al., 2022. Dysregulation of DNA methylation and epigenetic clocks in prostate cancer among puerto rican men. Biomolecules 12.
Burda, P., Laslo, P., Stopka, T., 2010. The role of PU.1 and GATA-1 transcription factors during normal and leukemogenic hematopoiesis. Leukemia 24, 1249–1257.
Celarain, N., Tomas-Roig, J., 2020. Aberrant DNA methylation profile exacerbates inflammation and neurodegeneration in multiple sclerosis patients. J. Neuroinflamm. 17, 21.
Cun-Yu, W., W, M.M., G, K.R., V, G.D., S, B.A., 1979. NF-κB Antiapoptosis: induction of TRAF1 and TRAF2 and c-IAP1 and c-IAP2 to suppress Caspase-8 activation. Science 281, 1680–1683, 1998.
Datta, De, D., Datta, A., Bhattacharjya, S., Roychoudhury, S., 2013. NF-kappaB mediated transcriptional repression of acid modifying hormone gastrin. PLoS One 8, e73409.
Diboun, I., Wani, S., Ralston, S.H., Albagha, O.M.E., 2021. Epigenetic analysis of Paget's disease of bone identifies differentially methylated loci that predict disease status. Elife 10, e65715.
Divisato, G., et al., 2016. ZNF687 mutations in severe paget disease of bone associated with giant cell tumor. Am. J. Hum. Genet. 98, 275–286.
Fedotova, A., Bonchuk, A., Mogila, V., Georgiev, P., 2017. C2H2 zinc finger proteins: the largest but poorly explored family of higher eukaryotic transcription factors. Acta Nat. 9, 47–58.
Foxler, D.E., et al., 2011. PU.1 is a major transcriptional activator of the tumour suppressor gene LIMD1. FEBS Lett. 585, 1089–1096.
Ganss, B., Jheon, A., 2004. Zinc finger transcription factors in skeletal development. Crit. Rev. Oral Biol. Med. 15, 282–297.
Gennari, L., Rendina, D., Falchetti, A., Merlotti, D., 2019. Paget's disease of bone. Calcif. Tissue Int. 104, 483–500.
Gennari, L., et al., 2022. Update on the pathogenesis and genetics of Paget's disease of bone. Front. Cell Dev. Biol. 10.
Handy, D.E., Gavras, H., 1996. Evidence for cell-specific regulation of transcription of the rat α2A-adrenergic receptor gene. Hypertension 27, 1018–1024.
Hayden, M.S., Ghosh, S., 2012. NF-κB, the first quarter-century: remarkable progress and outstanding questions. Genes Dev. 26, 203–234.
Héberlé, É., Bardet, A.F., 2019. Sensitivity of transcription factors to DNA methylation. Essays Biochem. 63, 727–741.
Imagawa, K., et al., 2014. Association of reduced type IX collagen gene expression in human osteoarthritic chondrocytes with epigenetic silencing by DNA hypermethylation. Arthritis Rheumatol. 66, 3040–3051.
Jiang, X., et al., 2018. The role of Sox9 in collagen hydrogel-mediated chondrogenic differentiation of adult mesenchymal stem cells (MSCs). Biomater. Sci. 6, 1556–1568.
Kamachi, Y., Kondoh, H., 2013. Sox proteins: regulators of cell fate specification and differentiation. Development 140, 4129–4144.
Kaplan, F.S., Singer, F.R., 1995. Paget's disease of bone: pathophysiology, diagnosis, and management. J. Am. Acad. Orthop. Surg. 3, 336–344.
Karpurapu, M., et al., 2014. Krüppel Like Factor 4 promoter undergoes active demethylation during monocyte/macrophage differentiation. PLoS One 9, e93362.
Kwon, O.H., Lee, C.-K., Lee, Y.I., Paik, S.-G., Lee, H.-J., 2005. The hematopoietic transcription factor PU.1 regulates RANK gene expression in myeloid progenitors. Biochem. Biophys. Res. Commun. 335, 437–446.
Lee, M.-H., et al., 2005. Dlx5 specifically regulates Runx2 Type II expression by binding to homeodomain-response elements in the Runx2 distal promoter. J. Biol. Chem. 280, 35579–35587.
Lee, T.I., Young, R.A., 2013. Transcriptional regulation and its misregulation in disease. Cell 152, 1237–1251.
Lefebvre, V., Dvir-Ginzberg, M., 2017. SOX9 and the many facets of its regulation in the chondrocyte lineage. Connect Tissue Res. 58, 2–14.
Lefebvre, V., Huang, W., Harley, V.R., Goodfellow, P.N., de, B., 1997. C. SOX9 is a potent activator of the chondrocyte-specific enhancer of the pro alpha1(II) collagen gene. Mol. Cell Biol. 17, 2336–2346.
Lin, B., et al., 2021. Transcription factor DLX5 promotes hair follicle stem cell differentiation by regulating the c-MYC/microRNA-29c-3p/NSD1 axis. Front. Cell Dev. Biol. 9.
Liu, L., Jin, G., Zhou, X., 2015. Modeling the relationship of epigenetic modifications to transcription factor binding. Nucleic Acids Res. 43, 3873–3885.
Mackeh, R., Marr, A.K., Fadda, A., Kino, T., 2018. C2H2-type zinc finger proteins: evolutionarily old and new partners of the nuclear hormone receptors. Nucl. Recept. Signal. 15, 1–22.
Novack, D.V., 2011. Role of NF-κB in the skeleton. Cell Res. 21, 169–182.
Oeckinghaus, A., Ghosh, S., 2009. The NF-kappaB family of transcription factors and its regulation. Cold Spring Harb. Perspect. Biol. 1, a000034.
Park-Min, K.H., 2017. Epigenetic regulation of bone cells. Connect Tissue Res. 58, 76–89.
Peacock, J.D., Huk, D.J., Ediriweera, H.N., Lincoln, J., 2011. Sox9 transcriptionally represses Spp1 to prevent matrix mineralization in maturing heart valves and chondrocytes. PLoS One 6, e26769.
Probst, A. v, Dunleavy, E., Almouzni, G., 2009. Epigenetic inheritance during the cell cycle. Nat. Rev. Mol. Cell Biol. 10, 192–206.
Ramanathan, B., Minton, J.E., Ross, C.R., Blecha, F., 2005. PU.1-mediated transcriptional regulation of prophenin-2 in primary bone marrow cells. Gene 352, 1–9.
Razin, S. v, Borunova, V. v, Maksimenko, O.G., Kantidze, O.L., 2012. Cys2his2 zinc finger protein family: classification, functions, and major members. Biochemistry 77, 217–226.
Reppe, S., et al., 2017. Distinct DNA methylation profiles in bone and blood of osteoporotic and healthy postmenopausal women. Epigenetics 12, 674–687.
Roberts, S.G.E., Green, M.R., 1995. Dichotomous regulators. Nature 375, 105–106.
Rong, H., et al., 2007. Eos, MITF, and PU.1 recruit corepressors to osteoclast-specific genes in committed myeloid progenitors. Mol. Cell Biol. 27, 4018–4027.
Rothenberg, E. v, Hosokawa, H., Ungerbäck, J., 2019. Mechanisms of action of hematopoietic transcription factor PU.1 in initiation of T-cell development. Front. Immunol. 10.
Rump, K., et al., 2019. DNA methylation of a NF-κB binding site in the aquaporin 5 promoter impacts on mortality in sepsis. Sci. Rep. 9, 18511.
Samee, N., et al., 2008. Dlx5, a positive regulator of osteoblastogenesis, is essential for osteoblast-osteoclast coupling. Am. J. Pathol. 173, 773–780.
Sharma, S., et al., 2020. Epigenetic and transcriptional regulation of osteoclastogenesis in the pathogenesis of skeletal diseases: a systematic review. Bone 138, 115507.
Shi, W., Zhou, W., 2006. Frequency distribution of TATA Box and extension sequences on human promoters. BMC Bioinform. 7.

Silva, I.A.L., et al., 2018. Effect of genetic variants of OPTN in the pathophysiology of Paget's disease of bone. Biochim. Biophys. Acta (BBA) Mol. Basis Dis. 1864, 143–151.
Tadic, T., et al., 2002. Overexpression of Dlx5 in chicken calvarial cells accelerates osteoblastic differentiation. J. Bone Miner. Res. 17, 1008–1014.
Theodorou, D.J., Theodorou, S.J., Kakitsubata, Y., 2011. Imaging of Paget disease of bone and its musculoskeletal complications: Review. Am. J. Roentgenol. 196, 64–75.
Tondravi, M.M., et al., 1997. Osteopetrosis in mice lacking haematopoietic transcription factor PU.1. Nature 386, 81–84.
Visconti, V.V., et al., 2021. DNA methylation signatures of bone metabolism in osteoporosis and osteoarthritis aging-related diseases: an updated review. Int. J. Mol. Sci. 22, 4244.
Vrtačnik, P., Marc, J., Ostanek, B., 2014. Epigenetic mechanisms in bone. Clin. Chem. Lab Med. 52, 589–608.
Wang, T., et al., 2017. The CpG dinucleotide adjacent to a κB site affects NF-κB function through its methylation. Int. J. Mol. Sci. 18, 528.
Xu, F., et al., 2021. The roles of epigenetics regulation in bone metabolism and osteoporosis. Front. Cell Dev. Biol. 8.
Yang, X., Karsenty, G., 2002. Transcription factors in bone: developmental and pathological aspects. Trends Mol. Med. 8, 340–345.
Zhang, W., Kone, B.C., 2002. NF-κB inhibits transcription of the H+-K+-ATPase α2-subunit gene: role of histone deacetylases. Am. J. Physiol. Ren. Physiol. 283, F904–F911.
Zhu, H., Tang, J., Tang, M., Cai, H., 2013. Upregulation of SOX9 in osteosarcoma and its association with tumor progression and patients' prognosis. Diagn. Pathol. 8, 183.